Predictive Modeling of Nonlinear Breakdown Voltage in Silicone Rubber Polymer Insulators with Fly Ash Filler Using the GLME and BPNN Methods

Davina Salmah An'nafri
Department of Electrical Power Engineering, Institut Teknologi Perusahaan Listrik Negara, Jakarta, Indonesia

Christiono
Department of Electrical Engineering, Institut Teknologi Perusahaan Listrik Negara, Jakarta, Indonesia

Miftahul Fikri
Department of Electrical Engineering, Institut Teknologi Perusahaan Listrik Negara, Jakarta, Indonesia

Nurmiati Pasra
Department of Electrical Engineering, Institut Teknologi Perusahaan Listrik Negara, Jakarta, Indonesia

Andi Dyah Harum
Department of Electrical Engineering, Institut Teknologi Perusahaan Listrik Negara, Jakarta, Indonesia

Abstract: The expansion of Indonesia's transmission and distribution network increases the demand for high-voltage insulator materials with reliable dielectric performance and sustainable manufacturing. Silicone rubber (SiR) filled with coal fly ash is a promising alternative; however, its breakdown voltage varies nonlinearly with filler composition, temperature, and fly ash source. This study proposes a complementary statistical machine learning framework using Generalized Linear Mixed Effects (GLME) for interpretable statistical analysis and a Backpropagation Neural Network (BPNN) for flexible nonlinear prediction. The analysis used 512 secondary observations from four Indonesian fly ash sources, with filler compositions of 10–80% and temperatures of 35–50°C. Breakdown voltage increased with fly ash content up to an optimum of approximately 60–65% before declining at higher loadings, while increasing temperature consistently reduced dielectric strength. GLME achieved $R^2 = 0.7457$, RMSE = 0.0354, and MAPE = 1.57%, whereas the five-fold cross-

Correspondents Author:
Christiono, Department of Electrical Engineering, Institut Teknologi Perusahaan Listrik Negara, Jakarta, Indonesia
Email: christiono@itpln.ac.id

Received June 28, 2025; Revised July 15, 2026; Accepted July 15, 2026; Published August 1, 2026.

validated BPNN showed slightly better average predictive performance, with R^2 = 0.7617, RMSE = 0.0343, and MAPE = 1.56%. GLME provides interpretable and statistically testable coefficients, whereas BPNN captures additional complex nonlinear patterns without requiring a predefined functional form. SEM and XRF characterization supported the observed nonlinear trends through particle dispersion and fly ash oxide composition, predominantly SiO_2 and Al_2O_3. The proposed complementary framework combines statistical interpretability with nonlinear predictive capability, supporting fly ash composition selection, efficient material screening, and breakdown voltage prediction for high voltage silicone rubber insulator applications.

Keywords: Breakdown voltage, Silicone Rubber, Fly Ash, Generalized Linear Mixed Effects.

Introduction

Indonesia's expanding electric power infrastructure, as projected under PLN's 2025–2034 Electricity Supply Business Plan (RUPTL), is expected to require substantial additions to transmission and distribution networks over the next decade, thereby increasing the demand for reliable, dielectrically robust, and cost-effective high-voltage insulation materials (Kementerian Energi dan Sumber Daya Mineral Republik Indonesia & PT PLN (PERSERO), 2025). Insulator failure can directly compromise power-supply continuity; therefore, insulation materials must provide adequate mechanical strength, high electrical resistivity, and stable dielectric performance under varying operating conditions to ensure long-term network reliability (Yousaf et al., 2022). Silicone rubber (SiR) polymer insulators are increasingly used as lightweight, UV-resistant, and cost-effective alternatives to conventional glass and ceramic insulators (Ahmad et al., 2025). Their dielectric and mechanical properties can be further enhanced by incorporating fly ash, a coal-combustion byproduct rich in silica (SiO_2), alumina (Al_2O_3), and other metal oxides, as a filler (Manjang et al., 2015). In addition to improving material performance, the utilization of fly ash as a filler provides a sustainable pathway for converting an abundant industrial waste stream into a value-added engineering material (Mathapati et al., 2021). Previous experimental studies have demonstrated the potential of fly ash to improve the electrical properties of SiR insulators (Manjang et al., 2015). SiR fly ash composites have shown comparatively stable performance under wet conditions, whereas similarly filled epoxy resins may experience deterioration due to increased water diffusion and relative permittivity (Kitta et al., 2016a). Increasing fly ash content has also been reported to improve permittivity and breakdown voltage up to an optimum composition, beyond which performance may decline due to aging and excessive filler loading (Kitta et al., 2016b). A previous quadratic regression study identified an optimum fly ash composition of approximately 50.88% for breakdown-voltage performance (R. Christiono et al., 2023). Furthermore, fly ash addition within an appropriate range can strengthen the internal composite structure and increase tensile strength, although excessive filler loading may reduce elongation because of increased material stiffness (Fikri et al., 2024). Breakdown voltage represents the voltage level at which an insulating material undergoes dielectric failure and is influenced by material composition, thickness, microstructure, and testing conditions, particularly temperature (Foruzan et al., 2018). Increasing temperature can enhance charge-carrier mobility and alter the material microstructure, thereby reducing dielectric strength in ceramic and composite-based insulating materials (C. Christiono et al., 2025; Li et al., 2024). In particulate-filled composites, filler fraction and environmental conditions can interact nonlinearly with electrical performance, often producing an optimum composition beyond which further filler addition becomes detrimental (Ren & Sancaktar, 2019). The oxide composition and morphological characteristics of the filler may further influence this behavior (Alterary & Marei., 2021). Despite these advances, most previous studies on fly ash-filled SiR have relied primarily on conventional regression models or standalone machine learning approaches. Conventional regression provides direct statistical interpretability but is constrained by a predefined functional form and may have limited flexibility in representing complex nonlinear relationships and source-specific heterogeneity. Conversely, machine learning models can capture nonlinear patterns with fewer assumptions about the underlying functional relationship, but they often operate as black-box models whose internal parameters have limited direct physical interpretation (Rudin., 2019). Recent machine learning applications to semiconductor and dielectric materials have demonstrated strong predictive capability, although many primarily emphasize prediction accuracy without providing a statistically interpretable explanation of the governing physical factors (Gallagher et al., 2024). Even recent interpretable machine learning approaches for polymer dielectric properties remain largely concentrated in electronics-material applications and have not been widely applied to filler-dependent breakdown-voltage prediction in high-voltage polymer insulator composites (He et al., 2025). This methodological gap motivates the complementary use of the Generalized Linear Mixed Effects (GLME) model and the Backpropagation Neural Network (BPNN) within a unified evaluation framework. GLME provides statistically interpretable estimates of the effects of temperature, fly ash composition, and source-specific variability through its fixed- and random-effects structure, whereas BPNN provides greater flexibility in capturing additional complex nonlinear patterns without requiring a predefined functional form. Rather than constituting a mathematically coupled hybrid model, the two approaches are developed independently and evaluated on the same underlying dataset, allowing statistical interpretability and nonlinear predictive capability to be assessed together.

This framework advances beyond previous fly ash SiR studies by directly benchmarking a mixed-effects statistical model against a cross-validated neural network while linking the resulting nonlinear trends to independent material characterization.

The GLME model extends conventional regression by simultaneously accommodating fixed and random effects, making it suitable for data with systematic experimental factors and grouped heterogeneity (Rohmaniah & Chandra., 2018; Stoffel et al., 2021). In this study, GLME is used to quantify the effects of temperature and fly ash composition while accounting for variation associated with different fly ash sources. In contrast, BPNN is employed to learn complex nonlinear relationships among the input variables and breakdown voltage (Fei et al., 2023; Permana & Nur Salisah, 2022). The two models are evaluated using the coefficient of determination (R^2), Root Mean Square Error (RMSE), and Mean Absolute Percentage Error (MAPE), which provide complementary measures of explained variance and prediction error (Chicco et al., 2021). Accordingly, this study aims to analyze the effects of fly ash composition and temperature on the breakdown voltage of SiR polymer insulators, model their nonlinear relationships using GLME, develop and cross-validate a BPNN-based prediction model, compare the complementary capabilities of both approaches using R^2, RMSE, and MAPE, and support the interpretation of the resulting nonlinear trends through independent SEM and XRF material characterization.

The main contributions of this study are as follows:

1. A complementary GLME BPNN modeling framework is proposed, combining statistically interpretable inference from GLME with flexible nonlinear prediction from BPNN for analyzing the breakdown voltage of fly ash-filled SiR insulators within a unified evaluation framework.

2. The nonlinear and interactive effects of temperature and fly ash composition are quantitatively investigated, while the GLME structure accounts for heterogeneity associated with four Indonesian fly ash sources.

3. GLME and BPNN are directly benchmarked using R^2, RMSE, and MAPE, clarifying the practical trade-off between statistical interpretability and nonlinear predictive flexibility.

4. The model-derived nonlinear trends are supported by independent SEM and XRF characterization, linking the observed electrical behavior to fly ash particle dispersion and oxide composition

Research Method

The overall research workflow, from data collection to statistical and machine learning modeling and material characterization, is summarized in Figure 1. Breakdown voltage data obtained from four fly ash sources, together with the corresponding temperature and filler composition variables, were first collected and log-transformed. Subsequently, the GLME and cross-validated BPNN models were independently developed using the transformed data and evaluated using R^2, RMSE, and MAPE. Finally, the nonlinear trends identified by both models were supported by SEM and XRF material characterization, which provided physical insights into particle dispersion and oxide composition.

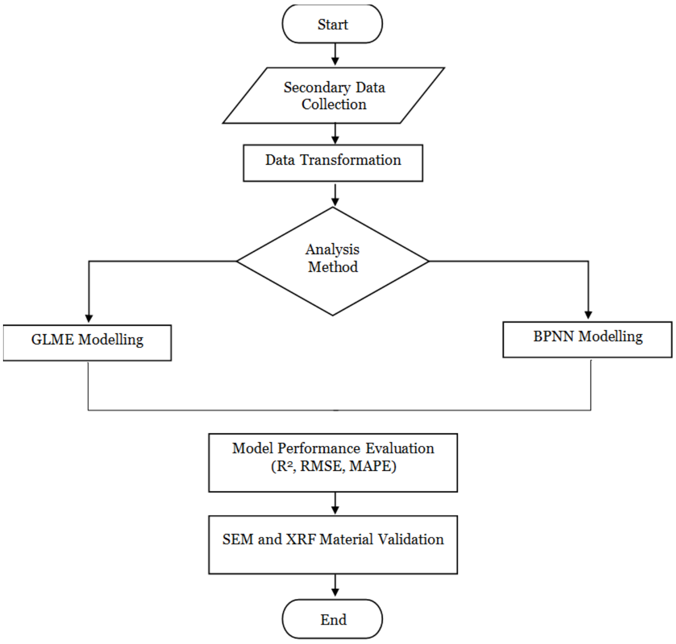

Figure 1 Overview of the research workflow, from secondary data collection and log-transformation, through parallel GLME and BPNN model development and five-fold cross-validation, to comparative performance evaluation and independent SEM/XRF material validation

Data Collection

This study used secondary data on the breakdown voltage of silicone rubber polymer insulators containing coal fly ash filler from four regions: fly ash from the Solusi Bangun Indonesia Cement Plant, Bekasi (FA-SBI); fly ash from the Suralaya Coal-Fired Power Plant, Banten (FA-PSC); fly ash from the Basowa Cement Plant, Pangkajene Islands (FA-PSB); and fly ash from the Paiton Power Plant, Probolinggo (FA-PPP). The fly ash filler composition varied at 10%, 20%, 30%, 40%, 50%, 60%, 70%, and 80%, and tests were conducted at 35°C, 40°C, 45°C, and 50°C with four replicates per condition, giving a total of 512 data points.

Data Transformation

To stabilize data variability and improve the linearity of the relationship between variables, thereby supporting a more effective modeling process (Lee., 2020), a logarithmic transformation was applied to the breakdown voltage values:

$$Y_{trans} = \log_{10}(Y) \tag{1}$$

Where Y_{trans} is the transformed value, and Y is the original breakdown voltage. This transformation compresses the data range and produces a more proportional distribution, supporting more effective analysis and modeling (West., 2022).

Generalized Linear Mixed Effects

Generalized Linear Mixed Effects (GLME) modeling was employed to analyze the relationship between temperature, fly ash composition, and the breakdown voltage of silicone rubber polymer insulators. GLME was selected because it can simultaneously estimate the effects of systematic explanatory variables through fixed effects while accounting for source-specific heterogeneity through random effects. In this study, temperature and fly ash composition were included as continuous fixed effects, while fly ash source (region) was included as a categorical fixed effect to quantify systematic differences among sources relative to a reference category. In addition, source-specific random intercepts and random temperature slopes were incorporated to account for residual variation in baseline breakdown voltage and temperature response among fly ash sources (Budhyanto et al., 2024; Sunandi et al., 2022). The GLME analysis was implemented in MATLAB R2024a using the Statistics and Machine Learning Toolbox. In general, the GLME model is expressed as:

$$g(\mu_{ij}) = X_{ij}\beta + Z_{ij}b_i \tag{2}$$

Where $g(\mu_{ij})$ is the link function, X_{ij} is the fixed effects design matrix, β is the vector of fixed effects parameters, Z_{ij} is the random effects design matrix, and b_i is the random effects vector. The specific GLME equation used in this study is:

$$\begin{aligned} BDV_{ij} = (\beta_0 + b_{0j}) + \beta(Region_i) + (\beta_2 + b_{1j})Temp_{ij} + \beta_3(Comp_{ij}) \\ + \beta_4(Comp_{ij}^2) + \beta_5(Temp_{ij} \times Comp_{ij}) + \varepsilon_{ij} \end{aligned} \tag{3}$$

The fixed effects structure in Equation (3), comprising region, temperature, composition, a quadratic composition term, and a temperature composition interaction, was selected based on the exploratory trends observed in Figures 2 and 3. These trends showed an approximately linear decrease in breakdown voltage with increasing temperature and a distinctly nonlinear rise-then-decline response to increasing filler composition. Therefore, the quadratic composition term was included as the simplest parametric extension capable of representing the observed interior optimum, while the temperature composition interaction was incorporated to evaluate whether the effect of filler composition on breakdown voltage varies with temperature. Source-specific random intercepts and random temperature slopes were included to account for potential differences among fly ash sources in both baseline breakdown voltage and temperature sensitivity. Random slopes were not included for the composition terms because the exploratory trends indicated a broadly similar composition-response pattern across the investigated sources; consequently, introducing additional random slopes would increase model complexity without clear exploratory evidence of improved model representation.

Backpropagation Neural Network (BPNN)

The Backpropagation Neural Network (BPNN) is a supervised learning method capable of modeling complex nonlinear relationships between input and output variables through iterative adjustment of network weights and biases (Fei et al., 2023). In this study, three input variables, temperature, fly ash composition, and fly ash source category, were used to predict breakdown voltage. The net input and output of neuron j are expressed as:

$$Z_j = \sum_{i=1}^{n} w_{ij} x_i + b_j \tag{4}$$

$$a_j = f(Z_j) \tag{5}$$

where x_i is the input variable, w_{ij} is the connection weight, b_j is the bias, Z_j is the net input to neuron j, and $f(Z_j)$ is the activation function. The hidden layers employed the hyperbolic tangent sigmoid activation function (tansig), expressed as:

$$f(Z) = \frac{1}{1 + e^{-z}} \tag{6}$$

Whereas the output layer used a linear activation function (purelin) suitable for continuous regression.

The BPNN employed a 3–15–10–1 feedforward architecture, with tansig activation functions in the two hidden layers and a purelin function in the output layer. The network was trained using Bayesian Regularization backpropagation (trainbr), with a maximum of 2000 epochs, a performance goal of 1×10^{-7}, and a fixed random seed of 10 for reproducibility. Since trainbr does not require a user-defined fixed learning rate, no separate learning-rate parameter was specified. The BPNN hyperparameters were empirically specified rather than selected through an exhaustive automated hyperparameter optimization procedure. The 3–15–10–1 architecture was adopted to provide sufficient nonlinear modeling capacity while maintaining moderate network complexity. The BPNN model was implemented in MATLAB R2024a using the Deep Learning Toolbox. Model generalization was evaluated using five-fold cross-validation. The 512 observations were randomly partitioned into five mutually exclusive folds; in each iteration, approximately 80% of the data were used for training and the remaining 20% for independent testing. To prevent information leakage, min–max normalization to the range of -1 to 1 was performed independently within each fold using parameters estimated exclusively from the training data. Performance was evaluated on the logarithmic scale using R^2, RMSE, MAPE, and Pearson's correlation coefficient. The pooled out-of-fold predictions from all five test folds were used as the primary basis for reporting overall BPNN predictive performance, while fold-specific metrics were additionally examined to assess performance stability across the cross-validation folds. A formal sensitivity or uncertainty analysis was not performed in this study. Instead, model robustness and generalization were assessed through five-fold cross-validation, fold-specific normalization, residual diagnostics, and evaluation of predictive performance across the five test folds. Formal uncertainty quantification and sensitivity analysis are recommended for future studies.

Model Performance Evaluation

Model performance evaluation measured each model's accuracy and suitability for predicting breakdown voltage using the coefficient of determination (R^2), Root Mean Square Error (RMSE), and Mean Absolute Percentage Error (MAPE). R^2 measures the model's ability to explain variation in the actual data (Chicco et al., 2021), RMSE measures the magnitude of the average prediction error based on squared errors (Willmott & Matsuura, 2005), and MAPE expresses the average prediction error as a percentage of the actual values (Khair et al., 2017). Models with higher R^2, lower RMSE, and MAPE are considered to have better predictive performance. These three metrics were selected because they are complementary rather than redundant: R^2 indicates the overall proportion of variance in breakdown voltage explained by each model, RMSE penalizes large deviations more heavily and is therefore sensitive to outliers, and MAPE expresses the error in a scale independent percentage form that is easier to interpret in an engineering context; relying on R^2 alone could mask a model that fits the bulk of the data well but performs poorly on a few critical points, whereas combining it with RMSE and MAPE gives a more complete picture of both the goodness of fit and the practical magnitude of the prediction error.

The evaluation parameter equation used is as follows:

$$RMSE = \sqrt{\frac{\sum(Y - Y')^2}{n}} \tag{7}$$

$$MAPE = \frac{1}{n}\sum_{i=1}^{n}\left|\frac{Y_i - Y'_i}{Y_i}\right| \times 100\% \quad (8)$$

$$R^2 = 1 - \frac{\sum_{i=1}^{n}(Y_i - Y'_i)^2}{\sum_{i=1}^{n}(Y_i - \bar{Y})^2} \quad (9)$$

Where Y_i is the actual breakdown voltage, Y' is the predicted breakdown voltage, $\bar{Y}$ is the average of the actual values, and n is the number of observed data points.

Result and Discussion

Data Collection and Transformation Results

The secondary data used in this study comprise breakdown-voltage measurements on silicone rubber polymer insulators with fly ash filler from four regions (FA-SBI, FA-PSB, FA-PSC, and FA-PPP), with filler concentrations from 10% to 80% and temperatures from 35°C to 50°C. Figure 2 visualizes the resulting breakdown-voltage characteristics.

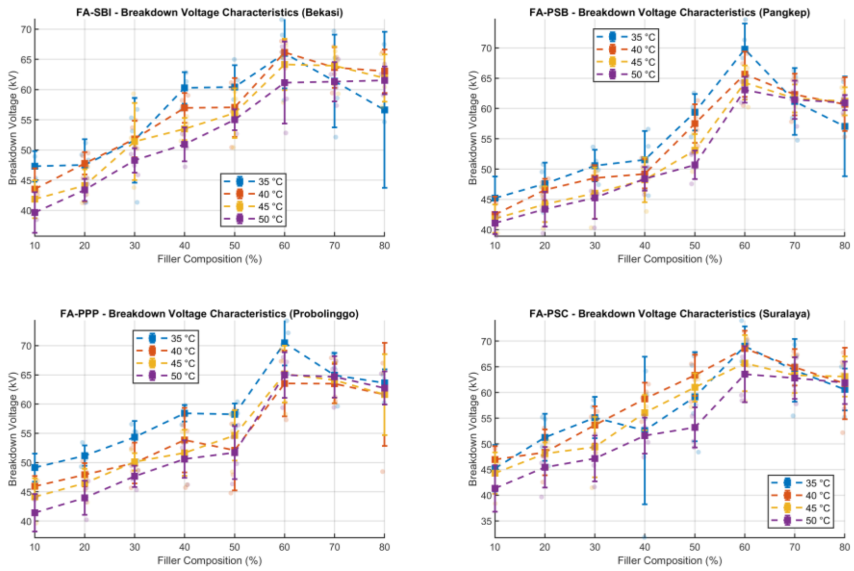

Figure 2 Breakdown Voltage of Silicone Rubber Insulators as a Function of Fly Ash Content and Temperature for Four Fly Ash Sources (FA-SBI, FA-PSC, FA-PSB, and FA-PPP)

As shown in Figure 2, the four fly ash sources generally exhibit an increasing breakdown-voltage trend as filler composition increases to approximately 60%, followed by a decrease or stabilization at higher filler contents of 70-80%. This nonlinear rise-then-decline behavior suggests that fly ash addition within an appropriate range enhances dielectric performance, whereas excessive filler loading may promote particle agglomeration and interfacial defects that limit further improvement. A consistent temperature effect is also observed, with the 35°C curves generally showing higher breakdown voltages than those at 40°C, 45°C, and 50°C, indicating that increasing temperature tends to reduce dielectric strength. This reduction may be associated with increased thermal energy and charge carrier mobility within the composite, which can facilitate electrical conduction and dielectric breakdown. Moreover, the nonuniform spacing and local fluctuations among the temperature curves at different filler compositions indicate that the combined effects of temperature and filler composition are not purely linear or additive, thereby supporting the use of nonlinear modeling approaches.

Before modeling, the breakdown-voltage data were logarithmically transformed (Equation 1) to reduce excessive variation, stabilize variance, and produce a more structured distribution, as shown in Figure 3.

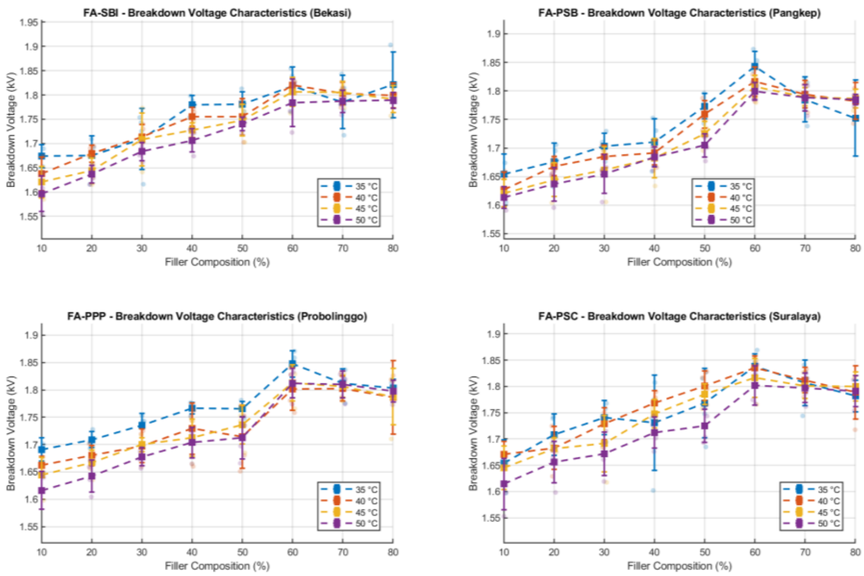

Figure 3 Logarithmically Transformed Breakdown Voltage as a Function of Fly Ash Content and Temperature for the Four Fly Ash Sources

Figure 3 shows that the qualitative relationships among filler composition, temperature, and breakdown voltage are preserved after the logarithmic transformation. Across the four fly ash sources, the breakdown voltage generally increases with filler composition up to approximately 60%, followed by a decrease or stabilization at higher filler contents. Compared with the original scale, the logarithmic transformation compresses the range of breakdown-voltage values and reduces the relative influence of extreme observations while preserving the underlying nonlinear trends. This transformation provides a more balanced numerical scale for subsequent GLME and BPNN modeling.

GLME Modelling

After fitting the GLME model, its fit was evaluated through residual diagnostics covering the normality of residuals, the distribution of residuals relative to fitted values, the stability of residual variance, and predictive accuracy, as shown in Figure 4.

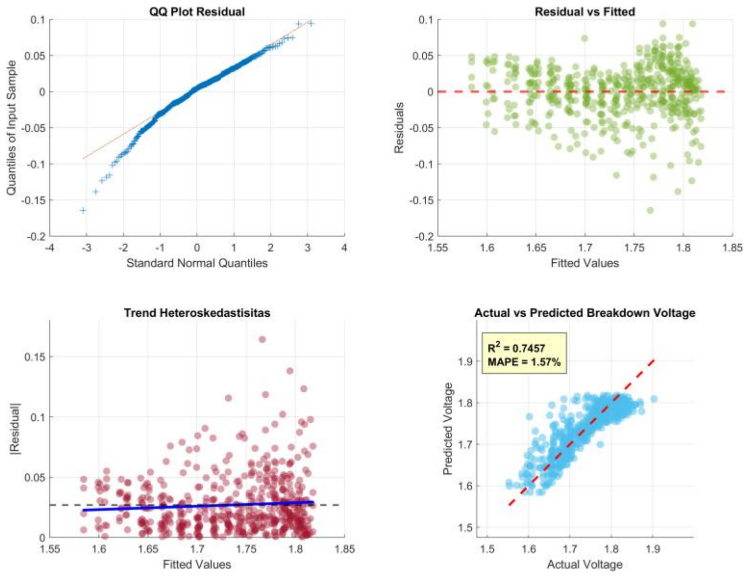

Figure 4 GLME model diagnostic plots: (a) residual QQ plot; (b) residual versus fitted values plot; (c) heteroscedasticity trend of absolute residuals against fitted values; and (d) actual versus predicted breakdown voltage on the logarithmic scale

Figure 4 presents the diagnostic evaluation and predictive performance of the GLME model. In Figure 4a, most residuals follow the reference line in the central portion of the QQ plot, although deviations are observed at both distribution tails, particularly in the lower tail. This pattern suggests that the residuals are approximately normally distributed in the central region, with some departures from normality at the extremes. Figure 4b shows that the residuals are generally scattered around the zero line without a strong systematic pattern, suggesting no substantial overall prediction bias, although greater dispersion is observed at higher fitted values. Consistently, Figure 4c indicates a slight increase in the magnitude of absolute residuals as the fitted values increase, suggesting mild heteroscedasticity rather than perfectly constant residual variance. Nevertheless, the overall residual pattern remains sufficiently stable for representing the general relationship among temperature, fly ash composition, fly ash source, and breakdown voltage. Finally, Figure 4d shows that the predicted values generally follow the diagonal reference line, with $R^2 = 0.7457$ and MAPE = 1.57%. These results indicate that the GLME model explains approximately 74.57% of the variation in log-transformed breakdown voltage while maintaining a relatively low average percentage prediction error.

To quantify the effect of each factor, parameter estimates, standard errors (SE), t-statistics, and p-values were obtained from the GLME model, summarized in Table 1.

Table 1 GLME Model Regression Coefficients for Breakdown Voltage ($\log_{10}$ scale)

Variable	Estimate	SE	tStat	p-Value
(Intercept)	1.7933	0.0450	39.88	<0.001
Pangkep_Region	-0.0148	0.0507	-0.29	0.7700
Probolinggo_Region	0.0018	0.0507	0.04	0.9718
Suralaya_Region	0.0086	0.0507	0.17	0.8661
Temperature	-0.0049	0.0006	-7.83	<0.001
Composition	0.0025	0.0006	4.09	<0.001
Temperature: Composition	0.00005	0.00001	4.44	<0.001
Composition^2	-0.00003	0.000003	-7.59	<0.001

Based on Table 1, temperature and fly ash composition significantly influenced breakdown voltage. The negative temperature coefficient ($\beta=-0.0049$, $p<0.001$) indicates that increasing temperature is associated with a reduction in breakdown voltage. This behavior may be attributed to increased thermal energy and charge-carrier mobility within the polymer matrix, which facilitates electrical conduction and dielectric breakdown. The positive linear composition coefficient ($\beta=0.0025$, $p<0.001$), together with the significant negative quadratic term ($\beta=-0.00003$, $p<0.001$), indicates a nonlinear rise-then-decline relationship between filler composition and breakdown voltage. Thus, increasing fly ash content initially improves dielectric performance up to an intermediate optimum, beyond which further filler addition leads to a decline in breakdown voltage. The significant temperature composition interaction ($\beta=0.00005$, $p<0.001$) further indicates that the effect of filler composition on breakdown voltage varies with testing temperature. The observed nonlinear composition response may be associated with changes in particle dispersion and filler matrix interfaces. At appropriate filler contents, dispersed fly ash particles may improve dielectric performance by increasing the complexity of potential conduction paths, whereas excessive filler loading may promote particle agglomeration and interfacial defects that facilitate local electric-field concentration and premature dielectric failure. This interpretation is supported by the SEM observations, which provide microstructural evidence of particle dispersion and agglomeration behavior at different filler concentrations.

The categorical regional coefficients were not statistically significant ($p>0.05$), indicating that systematic differences among the investigated fly ash sources were relatively small after accounting for temperature, composition, their nonlinear effects, and their interaction. The XRF results further showed that the investigated fly ash samples were predominantly composed of SiO_2 and Al_2O_3, with variations in their relative proportions among sources. This compositional similarity may partly explain the absence of statistically significant differences among the regional fixed effects. To further illustrate the effects of temperature and composition on breakdown voltage, the GLME predictions are visualized as characteristic curves in Figure 5.

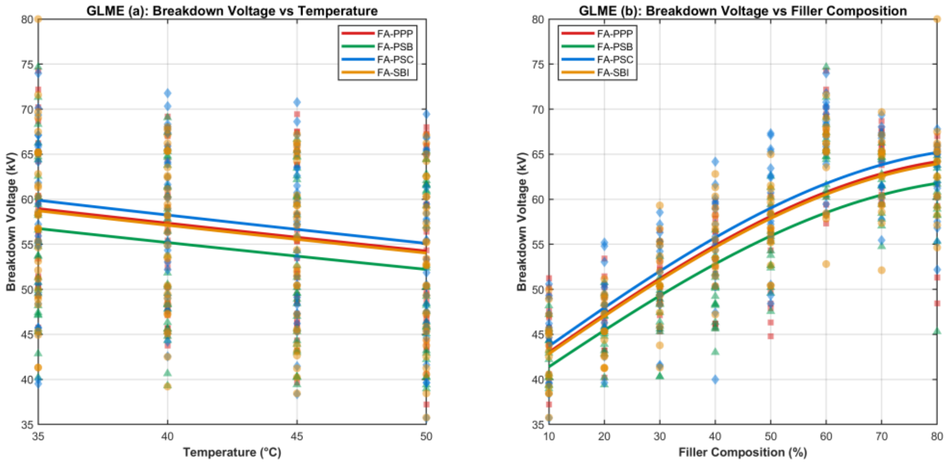

Figure 5 GLME-Predicted Breakdown Voltage Trends as a Function of (a) Temperature and (b) Fly Ash Composition for the Four Fly Ash Sources

Figure 5 illustrates the GLME predicted relationships between breakdown voltage, temperature, and filler composition for the four fly ash sources. In Figure 5a, breakdown voltage decreases approximately linearly with increasing temperature across all sources. The nearly parallel prediction curves indicate a broadly consistent negative temperature response, whereas the differences in curve elevation reflect source-specific variations captured by the GLME structure. In Figure 5b, breakdown voltage increases nonlinearly with filler composition, with the rate of increase gradually diminishing at higher filler contents. This concave-downward trend is consistent with the significant negative quadratic composition term reported in Table 1 and indicates a tendency toward saturation at higher filler loadings. The smooth GLME prediction curves represent the dominant overall relationships while reducing the influence of local fluctuations in the observed data. This characteristic enhances model interpretability but may limit the ability of GLME to capture localized nonlinear variations, which may partly explain its slightly lower predictive performance compared with BPNN. Differences in curve elevation among the four sources further indicate source-dependent variation while preserving a broadly similar overall composition response pattern.

BPNN Modeling

The predictive performance of the BPNN model was evaluated using five-fold cross-validation based on R^2, RMSE, MAPE, Pearson's correlation coefficient, and residual analysis. Figure 6 presents the agreement between actual and predicted values and the residual distribution based on pooled out-of-fold predictions from the five cross-validation folds.

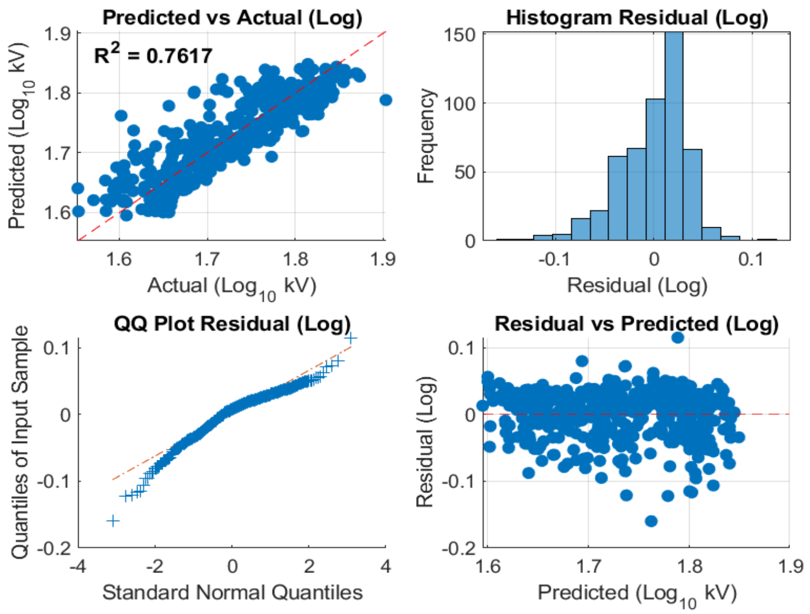

Figure 6 BPNN Model Diagnostic Plots: (a) Actual versus Predicted Breakdown Voltage, (b) Residual Histogram, (c) Residual QQ Plot, and (d) Residuals versus Predicted Values

The predictive performance of the BPNN model was evaluated using pooled out-of-fold predictions from five-fold cross-validation, as shown in Figure 6. In Figure 6a, the predicted values generally follow the ideal 1:1 line, with a pooled out-of-fold coefficient of determination of $R^2 = 0.7617$, indicating that the model explains approximately 76.17% of the variation in log-transformed breakdown voltage. Although some deviations occur at the extreme values, the overall distribution demonstrates a reasonably strong predictive relationship.

The residual histogram in Figure 6b is concentrated near zero, indicating relatively small prediction errors overall, although a longer negative tail suggests overprediction for several observations. The QQ plot in Figure 6c approximately follows the theoretical reference line in the central region but deviates at both tails, particularly the lower tail, indicating several relatively large prediction errors. Figure 6d shows that the residuals are generally distributed around zero without a pronounced nonlinear pattern, although greater dispersion and several negative residuals are observed at higher predicted values. Overall, these diagnostics indicate that the BPNN captures the dominant nonlinear structure of the data without evidence of severe systematic bias. The risk of overfitting was reduced through five-fold cross-validation, Bayesian Regularization (trainbr), and fold-specific normalization based exclusively on the training data. Nevertheless, the demonstrated generalization remains limited to the investigated temperature and filler composition ranges and the four fly ash sources included in the dataset. Compared with GLME, BPNN provides greater flexibility in capturing nonlinear patterns that may not be fully represented by the predefined quadratic and interaction terms of the statistical model, although at the cost of reduced direct interpretability.

To visualize these nonlinear relationships, the representative BPNN model from the best performing cross-validation fold was used to generate the continuous prediction curves shown in Figure 7, whereas the primary evaluation of predictive performance was based on the five-fold cross-validation results.

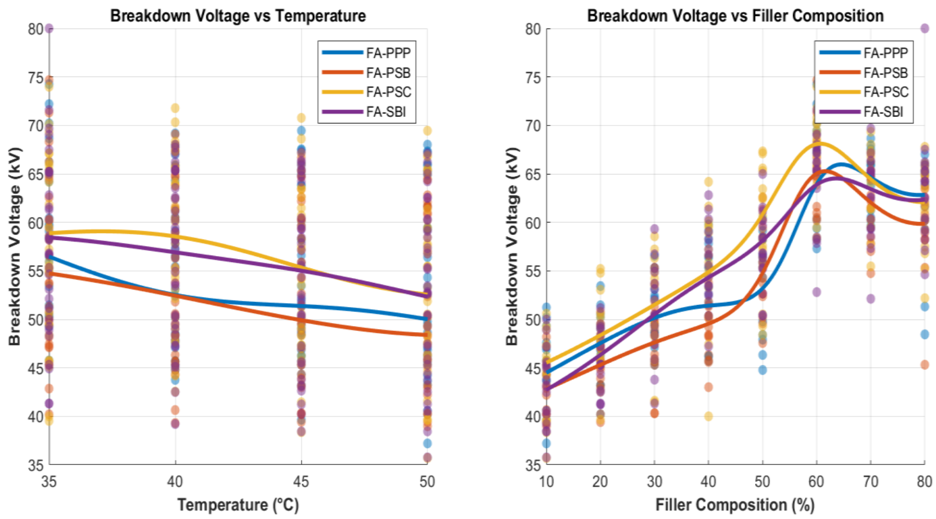

Figure 7 BPNN-Predicted Breakdown Voltage Trends as a Function of (a) Temperature and (b) Fly Ash Composition for the Four Fly Ash Sources

Figure 7 presents the predicted breakdown-voltage trends generated by the representative BPNN model from the best-performing cross-validation fold. As shown in Figure 7a, breakdown voltage generally decreases with increasing temperature across all four fly ash sources, although the slopes and curve shapes vary slightly among sources. This indicates that the BPNN captures source-dependent differences in the nonlinear temperature response. Compared with the nearly linear and parallel GLME prediction curves in Figure 5a, the BPNN curves exhibit greater flexibility in representing nonlinear variations among temperature, filler composition, and fly ash source, although this flexibility comes at the cost of reduced direct parameter interpretability. In Figure 7b, breakdown voltage generally increases with filler composition and reaches a predicted maximum at approximately 60–65%, followed by a decrease or stabilization at higher filler contents. The pronounced curvature around this range is consistent with the exploratory trends observed in the original data and demonstrates the ability of BPNN to capture localized nonlinear variations that are not fully represented by the smoother GLME curves in Figure 5b. While the GLME model identifies a concave-downward composition response with diminishing gains at higher filler contents, the BPNN more clearly reproduces the experimentally observed rise-then-decline pattern and locates the predicted optimum within the investigated range.

Model Performance Comparison

The results of the performance comparison between the GLME and BPNN models are presented in Table 2 below.

Table 2 Comparative Performance Evaluation of GLME and BPNN Models

Evaluation Parameters	GLME	BPNN
R^2	0.7457	0.7617
RMSE	0.0354	0.0343
MAPE (%)	1.57	1.56

Based on Table 2, the BPNN model demonstrated slightly better predictive performance than GLME, achieving a higher coefficient of determination (R^2 = 0.7617 versus 0.7457) and marginally lower prediction errors (RMSE = 0.0343 versus 0.0354; MAPE = 1.56% versus 1.57%). Although the differences are modest, the consistent improvement across all three metrics indicates that BPNN provides greater flexibility in capturing nonlinear patterns, whereas GLME offers directly interpretable and statistically testable coefficients.

The predictive performance obtained in this study is comparable to recent machine-learning applications in polymer dielectric materials and nanocomposites, although direct numerical comparison should be interpreted cautiously because of differences in datasets, material systems, and modeling approaches (He et al., 2025; Sun et al., 2025). The complementary use of GLME and BPNN is also consistent with recent developments in interpretable machine learning, which emphasize the importance of balancing predictive capability with transparent scientific interpretation (Zschech et al., 2026). More broadly, hybrid machine-learning frameworks have also demonstrated strong predictive capability in related high-voltage insulator applications; for instance, an IHHO-optimized XGBoost model achieved R^2 values above 0.99 in predicting insulator pollution severity from environmental data (Hamanah et al., 2025). While such tree-based ensemble approaches can achieve very high accuracy on well-structured environmental datasets, the present study's moderate R^2 range (0.75–0.76) reflects the inherently higher physical variability of breakdown voltage as a material property governed by microstructural and compositional factors rather than purely environmental conditions, underscoring the importance of complementing predictive accuracy with the interpretability offered by GLME. From an engineering perspective, the two models serve complementary purposes. GLME is useful for statistically interpreting the effects of temperature, filler composition, and fly ash source on breakdown voltage, while BPNN is better suited to flexible nonlinear prediction within the investigated data range. Thus, the proposed framework combines statistical interpretability with predictive flexibility, supporting material analysis and the screening of untested temperature–composition combinations. However, further validation using additional fly ash sources and broader experimental conditions is required to assess the external generalizability of both models.

SEM and XRF Validation

To support the modeling results obtained, validation was performed using Scanning Electron Microscopy (SEM) and X-Ray Fluorescence (XRF) analysis. SEM analysis was used to observe the morphology and distribution of fly ash particles in the silicone rubber matrix, while XRF analysis was used to identify the chemical composition of the fly ash.

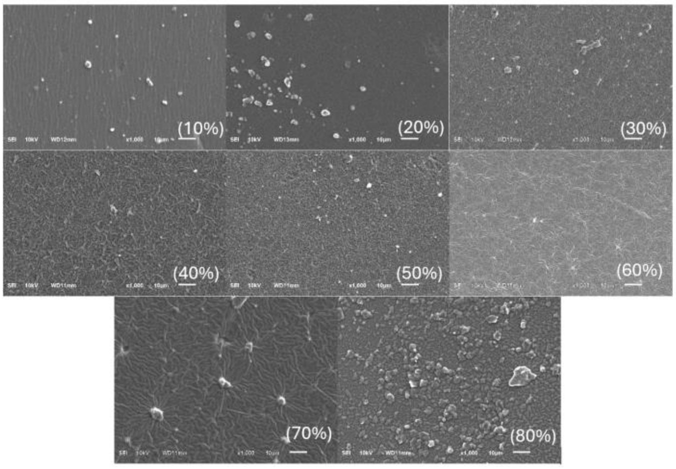

Figure 8 SEM Micrographs Showing Fly Ash Particle Dispersion in the Silicone Rubber Matrix at Low (10-20%), Intermediate (30-60%), and High (80%) Fly Ash Content

Based on Figure 8, at low fly ash contents (10–20%), the filler particles are unevenly distributed, and numerous voids are still observed within the silicone rubber matrix. Such an inhomogeneous microstructure may promote local electric-field concentration and reduce the dielectric strength of the composite. As the fly ash content increases to 30–60%, the filler particles become more uniformly dispersed, producing a denser microstructure with fewer voids. This more homogeneous distribution may improve interfacial interactions between the filler and polymer matrix, reduce local electric-field concentration, and enhance the dielectric strength of the composite, consistent with the higher breakdown voltage observed within this composition range. Conversely, at the highest fly ash content (80%), particle agglomeration becomes evident, leading to non-uniform filler dispersion and the formation of particle clusters. These agglomerated regions may act as defect sites that facilitate local electric-field concentration and dielectric failure, thereby contributing to the reduction in breakdown voltage at excessive filler contents. These morphological observations are consistent with the experimentally observed nonlinear breakdown-voltage trend and the BPNN prediction curves, while also supporting the concave-downward composition response indicated by the significant negative quadratic term in the GLME model.

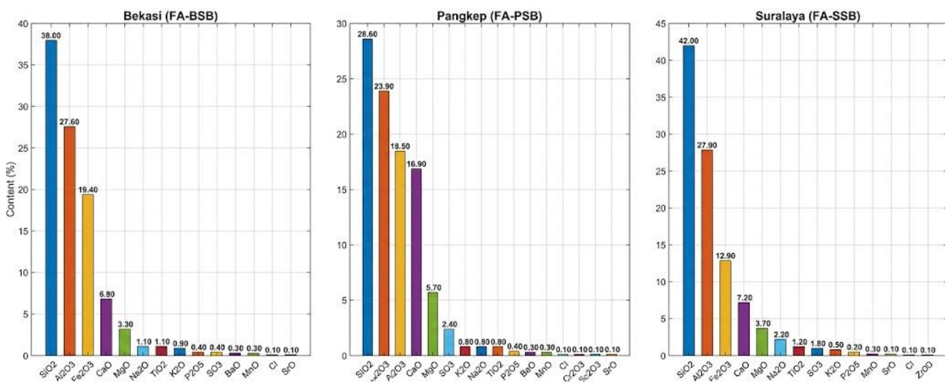

Figure 9 XRF-Determined Oxide Composition (SiO_2 and Al_2O_3) of Fly Ash from the Four Investigated Sources

Based on Figure 9, all fly ash samples were predominantly composed of SiO_2 and Al_2O_3, although their relative proportions varied among the different fly ash sources. The Suralaya sample exhibited the highest SiO_2 content (42.00%), followed by Bekasi (38.00%) and Pangkep (28.60%). The high concentrations of SiO_2 and Al_2O_3 are widely recognized as contributing to the dielectric performance of polymer composites because these oxides possess high electrical resistivity and can improve the insulating characteristics of the filler. Consequently, fly ash with higher oxide content is expected to contribute to better dielectric performance when uniformly dispersed within the silicone rubber matrix. Although differences in oxide composition were observed among the investigated fly ash sources, the GLME analysis indicated that these regional variations were not statistically significant after the effects of temperature and fly ash composition were considered. Therefore, the results suggest that filler composition and testing temperature exert a greater influence on breakdown voltage than differences in the chemical composition among the investigated fly ash sources.

Conclusions

This study investigated the nonlinear effects of temperature and fly ash composition on the breakdown voltage of silicone rubber polymer insulators using complementary GLME and BPNN modeling approaches. The results showed that increasing temperature generally reduced breakdown voltage, whereas increasing fly ash content improved dielectric performance up to an intermediate composition range before excessive filler loading led to diminishing or declining performance. The GLME model provided statistically interpretable information on the effects of temperature, composition, their interaction, and the significant negative quadratic composition term, achieving $R^2 = 0.7457$, RMSE = 0.0354, and MAPE = 1.57%. The BPNN demonstrated slightly better predictive performance, with $R^2 = 0.7617$, RMSE = 0.0343, and MAPE = 1.56%, and more clearly captured the nonlinear rise-then-decline trend with a predicted maximum at approximately 60–65% fly ash composition. SEM observations supported this behavior by showing improved particle dispersion at intermediate filler contents and pronounced agglomeration at excessive loading, while XRF characterization indicated that SiO_2 and Al_2O_3 were the predominant oxide components of the investigated fly ash sources. The main contribution of this study lies in the complementary evaluation of an interpretable mixed-effects statistical model and a flexible neural-network model within the same analytical framework. GLME provides statistically testable insight into the factors governing breakdown voltage, whereas BPNN offers greater flexibility for nonlinear prediction within the investigated data range. This framework can support material analysis and the screening of untested temperature composition combinations for fly ash filled silicone rubber insulators. However, the present findings are limited to 512 observations from four Indonesian fly ash sources under controlled experimental conditions. Future research should include additional fly ash sources, broader operating conditions, external validation datasets, and formal sensitivity and uncertainty analyses to assess model robustness and generalizability. Furthermore, benchmarking the proposed GLME BPNN framework against other advanced machine learning algorithms, such as Random Forest, XGBoost, and Support Vector Regression, would provide additional insight into the relative predictive advantages of tree-based, kernel-based, and neural network-based approaches for this class of dielectric composite problems.

References

Ahmad, S., Ahmed, R., Rahman, R. A., Ullah, A., Jamal, A., & Akram, R. (2025). A comprehensive study of nano/micro fillers on silicone rubber insulators: Electrical, mechanical, and thermal characterization. *Results in Engineering*, *25*.

https://doi.org/10.1016/j.rineng.2024.103654

Alterary, S. S., & Marei, N. H. (2021). Fly ash properties, characterization, and applications: A review. *Journal of King Saud University - Science*, *33*(6).

https://doi.org/10.1016/j.j ksus.2021.101536

Budhyanto, J. D., Saputra, K. V. I., Margaretha, H., & Ferdinand, F. V. (2024). Generalized Linear Mixed Models for Predicting Non-Life Insurance Claims. *INFERENSI*, *7*(2), 141. https://doi.org/10.12962/j27213862.v7i2.20447

Chicco, D., Warrens, M. J., & Jurman, G. (2021). The coefficient of determination R-squared is more informative than SMAPE, MAE, MAPE, MSE and RMSE in regression analysis evaluation. *PeerJ Computer Science*, *7*, 1–24. https://doi.org/10.7717/PEERJ-CS.623

Christiono, C., Romadhoni, M. L., Fikri, M., Zainal, D. M. P., & Iklas, K. A. (2025). Effect of Temperature on the Dielectric Properties of Silicone Rubber Polymer Insulator Filled With Coal Fly Ash. *2025 5th International Conference on High Voltage Engineering and Power Systems (ICHVEPS)*, 606–611.

https://doi.org/10.1109/ICH VEPS66 913.2 025. 11351258

Christiono, R., Iwa Garniwa M, K., Fikri, M., Thahara, A. A., & Putra, R. P. (2023). Optimization of Coal Fly Ash Filler Effect on Polymer Silicone Rubber Base Insulator Material on Dielectric Performance. *2023 4th International Conference on High Voltage Engineering and Power Systems (ICHVEPS)*, 705–710.
https://doi.org/10.1109/ICHVEPS58902.2023.10257370

Fei, R., Guo, Y., Li, J., Hu, B., & Yang, L. (2023). An Improved BPNN Method Based on Probability Density for Indoor Location. *IEICE Transactions on Information and Systems*, *E106.D*(5), 773–785.
https://doi.org/10.1587/transinf.2022DLP0073

Fikri, M., Christiono, Iwa Garniwa, M. K., Abduh, S., Sari, K. J., Raafid, H., An'nafri, D. S., & Romadhoni, M. L. (2024). The Effect of Addition of Coal Fly Ash as Filler in Silicone Rubber Polymer Isolator Materials on the Characteristics of Tensile Strength and Elongation. *ICT-PEP 2024 - International Conference on Technology and Policy in Energy and Electric Power: Resilient Power Systems: Navigating the Clean Energy Transition, Proceedings*, 166–169.
https://doi.org/10.1109/ICT-PEP63 827.2024.1 0733400

Foruzan, E., Akmal, A. A. S., Niayesh, K., Lin, J., & Sharma, D. D. (2018). Comparative study on various dielectric barriers and their effect on breakdown voltage. *High Voltage*, *3*(1), 51–59. https://doi.org/10.1049/hve.2017.0032

Gallagher, J. C., Mastro, M. A., Jacobs, A. G., Kaplar, Robert. J., Hobart, K. D., & Anderson, T. J. (2024). Detecting defects that reduce breakdown voltage using machine learning and optical profilometry. *Scientific Reports*, *14*(1), 7440.
https://doi.org/10.1038/s41598-024-57875-5

Hamanah, W. M., Al-Shammaa, A. A., Salem, A. A., Al-Wajih, E., Al-Soufi, K., & Farh, H. M. H. (2025). Hybrid machine learning predictions of high voltage polymeric insulator pollution. *Scientific Reports*, *15*(1), 42693.
https://doi.org/10.1038/s41598-025-26864-7

He, X., Wan, J., Zhang, S., Zhang, C., Xiao, P., Zheng, F., & Lu, Q. (2025). Interpretable Machine Learning Prediction of Polyimide Dielectric Constants: A Feature-Engineered Approach with Experimental Validation. *Polymers*, *17*(12), 1622.
https://doi.org/10. 3390/polym17121622

Kementerian Energi dan Sumber Daya Mineral Republik Indonesia, & PT PLN (PERSERO). (2025). *Rencana Usaha Penyediaan Tenaga Listrik (RUPTL) 2025-2034*.

Khair, U., Fahmi, H., Hakim, S. Al, & Rahim, R. (2017). Forecasting Error Calculation with Mean Absolute Deviation and Mean Absolute Percentage Error. *Journal of Physics: Conference Series*, *930*(1). https://doi.org/10.1088/1742-6596/930/1/012002

Kitta, I., Manjang, S., Tjaronge, W., & Irmawaty, R. (2016a). Effect of Coal Fly Ash Filler in Silicone Rubber and Epoxy Resin as Insulating Material in Wet Environmental Conditions. *International Journal of Mechanical & Mechatronics Engineering IJMME-IJENS*, *16*(2).

Kitta, I., Manjang, S., Tjaronge, W., & Irmawaty, R. (2016b). Effect of Fly Ash Filler Quantity on Electrical Properties of Silicone Rubber Insulator Material. *ARPN Journal of Engineering and Applied Sciences*, *11*(7).

www.arpn journals.com

Lee, D. K. (2020). Data transformation: A focus on the interpretation. *Korean Journal of Anesthesiology*, *73*(6), 503–508. https://doi.org/10.4097/kja.20137

Li, X., Liu, X., Ru, J., Zeng, Z., Bian, H., Li, Y., Zhong, H., & Chen, L. (2024). Effect of Thickness on the Breakdown Characteristics of Organic Insulation Materials under Microsecond Pulse Voltage. *Energies*, *17*(14). https://doi.org/10.3390/en17143538

Manjang, S., Pratama Putera, R., Syam Akil, Y., & Kitta, I. (2015). Electrical And Mechanical Properties of Fly Ash Filled Silicone Rubber for High Voltage Insulator. *ARPN Journal of Engineering and Applied Sciences*, *10*(17). www.arpnjournals.com

Mathapati, M., Amate, K., Prasad, C. D., Jayavardhana, M. L., & Raju, T. H. (2021). A review on fly ash utilization. *Materials Today: Proceedings*, *50*, 1535–1540.

https://doi.org/10.1016/j.matpr.2021.09.106

Permana, I., & Nur Salisah, F. (2022). The Effect of Data Normalization on the Performance of the Classification Results of the Backpropagation Algorithm. *IJIRSE (Indonesian Journal of Informatic Research and Software Engineering)*, *2*(1).

Ren, X., & Sancaktar, E. (2019). Use of fly ash as eco-friendly filler in synthetic rubber for tire applications. *Journal of Cleaner Production*, *206*, 374–382.

https://doi.org/ 10.1016/j.jclepro.2018.09.202

Rohmaniah, S. A., & Chandra, N. E. (2018). Perhitungan Premi Asuransi Jiwa Menggunakan Generalized Linear Mixed Models. *Jurnal Ilmiah Teknosains*, *4*(2). www.hrsonline.isr.umich.edu

Rudin, C. (2019). Stop explaining black box machine learning models for high stakes decisions and use interpretable models instead. *Nature Machine Intelligence*, *1*(5), 206–215. https://doi.org/10.1038/s42256-019-0048-x

Stoffel, M. A., Nakagawa, S., & Schielzeth, H. (2021). partR2: Partitioning R2 in generalized linear mixed models. *PeerJ*, *9*. https://doi.org/10.7717/peerj.11414

Sun, K., Yu, K., Du, X., Yang, R., Zhang, W., Lv, F., Fan, S., & Yu, X. (2025). Machine learning to explore nanocomposites with high dielectric strength by tailoring filler parameters. *Journal of Materials Science*, *60*(25), 10369–10379.

https://doi.org/10.1007/s10853-025-11077-0

Sunandi, E., Notodiputro, K. A., & Sartono, B. (2022). A study of generalized linear mixed model for count data using hierarchical bayes method. *Media statistika*, *14*(2), 194–205. https://doi.org/10.14710/medstat.14.2.194-205

West, R. M. (2022). Best practice in statistics: The use of log transformation. *Annals of Clinical Biochemistry*, *59*(3), 162–165. https://doi.org/10.1177/00045632211050531

Willmott, C. J., & Matsuura, K. (2005). Advantages of the mean absolute error (MAE) over the root mean square error (RMSE) in assesing average model performance. *CLIMATE RESEARCH*, *30*, 79–82. www.int-res.com

Yousaf, M., Iqbal, T., Hussain, M. A., Tabish, A. N., Haq, E. U., Siddiqi, M. H., Yasin, S., & Mahmood, H. (2022). Microstructural and mechanical characterization of high strength porcelain insulators for power transmission and distribution applications. *Ceramics International*, *48*(2), 1603–1610. https://doi.org/10.1016/j.ceramint.2021.09.239

Zschech, P., Weinzierl, S., & Kraus, M. (2026). Inherently Interpretable Machine Learning: A Contrasting Paradigm to Post-hoc Explainable AI. *Business & Information Systems Engineering*, *68*(2), 445–463. https://doi.org/10.1007/s12599-025-00964-0